

Full Length Article

Production of upgraded fuel blend from fast pyrolysis bio-oil and organic solvent using a novel three-stage catalytic process and its combustion characteristics in a diesel engine

Jude A. Onwudili^{a,b,*}, Vikas Sharma^{a,c}, Cristiane A. Scaldaferrri^a, Abul K. Hossain^{a,c}

^a Energy and Bioproducts Research Institute, School of Infrastructure & Sustainable Engineering, College of Engineering and Physical Sciences, Aston University, Birmingham B4 7ET, UK

^b Department of Chemical Engineering & Applied Chemistry, School of Infrastructure & Sustainable Engineering, College of Engineering and Physical Sciences, Aston University, Birmingham B4 7ET, UK

^c Department of Mechanical, Biomedical & Design Engineering, School of Engineering & Technology, College of Engineering and Physical Sciences, Aston University, Birmingham B4 7ET, UK



ARTICLE INFO

Keywords:

Catalytic bio-oil upgrading
Hydrocarbon biofuel
Hydrogen
Combustion
Emission
Fuel blend

ABSTRACT

An interdisciplinary approach involving the production and engine testing of a fuel blend containing upgraded bio-oil and fossil-derived solvent has been investigated in this present study. First, a novel 3-stage process of solvent-assisted catalytic upgrading of fast pyrolysis bio-oil was used to obtain a fuel blend with nearly 18 vol% biofuel content. Upgrading reactions were carried out between 160 °C and 300 °C, with 10 bar hydrogen gas, using 5 wt% Pt/Al₂O₃ catalyst for each of the three stages, with the main conversion reactions occurring in the first stage. The upgrading process produced 21.8 wt% of hydrocarbon-rich biofuel on bio-oil basis, achieving a high degree of deoxygenation with only 0.19 wt% oxygen in the final product. This was followed by the study of its combustion and emission characteristics in a 3-cylinder diesel engine, using a 10 vol% biofuel content in kerosene. All relevant testing regimes for liquid fuels were carried out, with its combustion and emission characteristics showing superior or similar results to those of conventions kerosene and diesel. The tested biofuel blend showed 2 % increments in engine performance. Overall, this work represents a significant advancement in the production of green liquid hydrocarbon-rich fuels for transport and domestic uses.

1. Introduction

Before the COVID-19 Pandemic, global fossil fuel consumption increased nearly steadily from 40,000 terawatt- hours (TWh) in 1965 to 136,000 TWh in 2019 [1], showing that in many countries around the world fossil fuel use continues to rise. For example, in the USA, the world's larger energy consumer, fossil fuel consumption between 1965 and 2019 fossil fuel consumptions increased from almost 14,000 to nearly 22,000 TWh per year [1,2]. While there have been many developments in alternative energy sources for stationary power generation (wind, solar, tidal etc) fossil fuel consumption, especially for the transport sector, continues to increase in many countries of the world. As the world's largest economy and highest energy consumer, the USA annual electricity generation from fossil fuels increased from 858 TWh in 1965 to 2590 TWh in 2019, albeit down from the peak generation of

3,000 TWh in 2007 [3].

The journey towards Net Zero has seen many developments around the electrification of transport but fossil fuels remain the dominant energy source for transport. Recent statistics on the purchase of new passenger vehicles in the UK in 2019 show that 63 % were petrol, 27 % diesel, 7 % full hybrid, <2% battery, <2% plug in hybrid [2]. Although the uptake of electric road vehicles is increasing, the overall energy mix of fossil fuels to electric (and/or hydrogen) is unlikely to change substantially over the next few years. Moreover, other forms of transport (for example aircraft and seacraft) are substantially behind road vehicles in the deployment of electric alternatives to fossil fuels. However, while technological advancement has ensured that carbon emissions have not increased in line with air traffic increases (kgCO₂ per revenue passenger kilometre 1960–2018 decreased 11-fold) [2], there is a continuing need to find replacements or substitutes for liquid fossil fuels to mitigate

* Corresponding author at: Energy and Bioproducts Research Institute, School of Infrastructure & Sustainable Engineering, College of Engineering and Physical Sciences, Aston University, Birmingham B4 7ET, UK.

E-mail address: j.onwudili@aston.ac.uk (J.A. Onwudili).

<https://doi.org/10.1016/j.fuel.2022.127028>

Received 13 October 2022; Received in revised form 26 November 2022; Accepted 28 November 2022

Available online 13 December 2022

0016-2361/© 2022 The Author(s). Published by Elsevier Ltd. This is an open access article under the CC BY license (<http://creativecommons.org/licenses/by/4.0/>).

environmental concerns.

One such potential replacement or substitute is lignocellulosic biomass pyrolysis oil or bio-oil which is obtained by heating dried biomass under oxygen-free or air-free or non-oxidizing conditions in a reactor. Lignocellulosic biomass feedstocks typically comprise wood and plant residues. The products of this pyrolysis process are solid (biochar), liquid (bio-oil) and gaseous (syngas) but the process conditions can be tuned to favour any of the three products. To obtain high bio-oil yields, fast pyrolysis of biomass which occurs at fast heating rates, short vapour residence times and moderate temperatures around 500 °C is used. Although the process is carried out in the absence of oxygen, bio-oils normally contain high levels of oxygen from the oxygen content of the biomass feedstock, which can be between 40 and 50 % by weight [4,5]. This level of oxygen in bio-oils makes them different to pure hydrocarbons derived from fossil fuels, resulting in poor volatility, high viscosity, corrosiveness, immiscibility with fossil fuels, thermal instability, and a tendency to polymerize when exposed to air and during storage [6]. Bio-oils exiting the pyrolysis reactor also contain relatively large amounts of water, most times more than 20 wt% [7].

Due of the chemical nature and physical properties of pyrolysis bio-oil there is no current substantial commercial market for it, although bio-oil can be used in boilers and furnaces. Bio-oil can replace or be blended with fossil-derived liquid fuels through the process of upgrading. The main targets of any bio-oil upgrading method involve not only oxygen removal but also the control of carbon chain lengths to be within those of commercial fossil fuels, such as gasoline, kerosene and diesel [8]. There are many methods which have been proposed for upgrading bio-oils, of which a thermal treatment and hydroprocessing are the most common [5,9]. Hydrodeoxygenation (HDO) is the term frequently used to describe the chemical process which uses heat and hydrogen gas or a hydrogen source (pressures of up to 100 bar) to remove oxygen from the bio-oil [10,11].

However, current HDO processes rely on large amounts of excess hydrogen which can increase processing costs and under certain conditions, can result in extensive carbon loss from the bio-oil due to char formation [12,13]. Accordingly, conventional HDO typically results in low yields of upgraded biofuel, is expensive and requires equipment capable of handling the high pressures of hydrogen required. Low pressure hydrogen solutions have been proposed using a molybdenum oxide catalyst, but these were either at very small scale, did not lead to total deoxygenation or suffer from excessive char formation [12,13]. Therefore, it would be highly beneficial for a new upgrading process which did not suffer from one or more of the problems of currently developed methods. The successful use of a two-stage continuous upgrading process has been reported by Abdullah et al. [14] to give a clear hydrocarbon-rich liquid product from bio-oil at a yield 19.6 wt% (dry biomass basis). However, the first stage led to extensive coke formation and deposition on the catalyst, which could affect ideal continuous processing through reactor plugging, catalyst deactivation or change the reaction selectivity towards the desired fuel production.

There are numerous studies on the combustion of raw and upgraded bio-oils in compression ignition engines to investigate fuel performance and exhaust emissions [4,7,8]. These have involved the blending of bio-oil or its upgraded version with conventional fossil fuels (gasoline, kerosene and diesel) or biofuels (bioethanol and biodiesel). However, several difficulties have been reported from these tests including the need to pre-heat bio-oil, long ignition delays, problematic engine start-up, operational instability, extensive coke depositions, inside the piston and cylinders, short combustion duration, various degrees of corrosion and clogging of injectors, and eventual engine failure [4,9]. To get round these challenges, very costly and complex engine modifications are often required, which may include the use of specialised spark ignition systems for start-up, running dual fuel systems, using corrosion resistant injectors, using low amounts of bio-oil in fuel blends and increasing the compression ratio [10].

Szwaja et al. [15], investigated *n*-butanol/pyrolysis oil blend on the

single-cylinder SI engine at a compression ratio of 11:1 for engine performance and combustion analysis. The blends of *n*-butanol and pyrolysis oil were made at two different volume ratios: 3:1 (25 %) and 1:1 (50 %) respectively. The combustion phases of butanol-pyrolysis oil blend were found to burn slowly. However, HC emission rose with pyrolysis oil raised to 50 % in a mix; but NO emissions were reduced by 20 %. The CO emission was observed similarly to the testing reference fuels (Gasoline E95). It was discovered that pyrolysis oil blended with *n*-butanol at a 3:1 ratio can be used as the engine's fuel with success. As a result, the engine can operate at a greater compression ratio without experiencing any combustion knock-related issues. Another study on Cottonseed pyrolysis oil (CPO)-diesel mix optimization on a water-cooled, one cylinder diesel engine was explored by Rajamohan et al. [16]. They used an intermediate pyrolysis process in a fixed-bed reactor to create pyrolysis oil. The engine operating condition was optimised using the response surface method (RSM) method. The highest BTE for the 5 % CPO and 95 % diesel fuel blend is 29.73 % at CR 18:1 and 100 % engine load. Lower HC and CO emissions were to 34 ppm and 0.01 %, respectively, at the same operating condition. CR 16:1 with 50 % engine load had the lowest NOx emission, which was measured at 106 ppm. Prasad et al. [17] produced a bio-oil from the tomato peel waste through pyrolysis. This tomato peel pyrolysis oil (TPO) was blended with diesel (5 %, 15 % and 25 %) and tested in diesel engine to evaluate the engine combustion, emissions, and performance. They reported that TPO5% blend shows 7–10 % higher brake thermal efficiency (BTE) than diesel fuel at full engine load. TPO25% blend shows higher heat release rate which increased the NOx emission about 5–8 % due to increases the oxygen %. Higher percentage of oxygen improve the combustion and increased in-cylinder temperature. The CO₂ increased (8–13 %) with increases the blend % than diesel fuel due to higher rate of CO oxidation at high temperature.

Blending bio-oil with fossil fuels has its own challenge, particularly due to poor miscibility; hence emulsifying agents are often used to enhance this property and increase the amount of bio-oil in the blend. The presence and ratio of the emulsifying agents may cause other problems in engine performance and emissions. In addition, due to low yields, it is difficult to make sufficient amount of upgraded bio-oils for engine testing. Therefore, requiring blending with commercial liquid fuels to achieve representative results. Hence, the addition of hydrocarbon fuels or their components prior to bio-oil upgrading may provide an advantage in terms of increasing the yields of upgraded bio-oil, enhancing miscibility of the blend and producing an engine-ready liquid fuel with significant biofuel content for engine testing and applications.

In this work, the application of a three-stage method for a solvent-assisted catalytic upgrading of fast pyrolysis bio-oil has been successfully used to produce an upgraded fuel blend consisting of biofuel from fast pyrolysis bio-oil and a thermally stable hydrocarbon solvent. These initial pieces of work were carried out with a stirred batch reactor at temperatures between 160 °C and 300 °C, under a low hydrogen pressure of 10 bar. The results presented here are based on extensive research programme (awaiting Patent application) that culminated in an optimised process to produce an upgraded liquid fuel blend containing more than 10 wt% of biofuel. The product has been characterised for its fuel properties and tested in an internal combustion engine. The performance of the upgraded fuel blend and its emissions have been compared with those of commercial kerosene and diesel fuels.

2. Experimental

2.1. Materials

The entire work was carried out from one batch of fast pyrolysis (FP) bio-oil (single-phase liquid) obtained from BTG Bioliquids, The Netherlands and kept in refrigerated storage. The bio-oil was characterised in-house and used directly without further purification. The FP bio-oil contained 29.7 wt% water. Dodecane (99 % purity) was

purchased from Fisher Scientific, Leicester, UK and used as received. Dodecane was selected due to its thermal stability at temperatures below 327 °C [18]. Commercial platinum metal catalyst (5 wt%), supported on 1 mm gamma alumina spheres (Pt/ γ -Al₂O₃) was obtained from Catal International ltd, based in Sheffield, UK.

The catalyst, in the form of 1 mm spheres, was reduced with H₂ gas at flow rate of 40 mL min⁻¹ flow rate in a tubular oven for 4 h at 200 °C according to the procedure reported by [19]. After the reduction procedure, the heating was stopped and the H₂ gas allowed to continuously flow over the catalysts to cool it down to room temperatures. While noble metal catalysts supported on carbon (e.g., Pt/C), have been found effective for HDO [20,21], they are not easily regenerated by calcination, unlike those supported on metal oxides or zeolites (e.g. alumina, silica). Hence, gamma alumina-supported Pt has been used in this study. Table 1 shows some of properties of the ‘as received’, reduced, used and regenerated (by calcination and reduction) Pt/Al₂O₃ catalyst (See Table 2).

2.2. FP bio-oil upgrading experimental set up

The schematic of the experimental procedure is shown in Fig. 1, based on the optimum conditions to maximise the yields of upgraded biofuel (Supplementary Information Table SI1). Processing of the FP bio-oil was carried out in three stages. The loading and unloading of the reactor and other post-reaction procedures were carried out in a fume cupboard. After loading the FP bio-oil, solvent and catalysts, the reactor was purged with a gentle stream of nitrogen at a flow rate of 10 mL min⁻¹, for 10 min to remove any trapped air before being pressurised with 10 bar hydrogen for the hydroprocessing reactions.

In the First Stage, 60 g of feedstock, comprising of 40 wt% FP bio-oil and 60 wt% dodecane (solvent) were reacted with 10 bar H₂ in contact with 5 g of Pt/Al₂O₃ catalyst. The reaction was carried out in a 450 mL Parr reactor (Parr Instrument Company, USA) equipped with a magnetic drive stirrer, water-cooled solenoid, a 1 kW electric heater, temperature controller and digital temperature, pressure gauge and electronic pressure readout. The reactor used consisted of detachable vessel and head, held together by a Split-Ring with compression bolts for moveable vessels. The empty reactor vessel weighed 1913.55 ± 0.04 g and the head weighed 3875.64 ± 0.02 g. The reactor loading was carried out using a VWR weighing balance VWR1611-3472 Model LP-6292i, with a maximum load of 6200 g and precision of 0.01 g. The liquid feedstock (FP bio-oil and solvent) was loaded into a glass liner, that fitted exactly into the inner dimensions of the reactor vessel. The glass liner was used to prevent any catalytic effects of the reactor materials. The reactor and its contents were heated at a rate of 12 °C min⁻¹ to 160 °C for 3 h and then to 300 °C for another 3 h with stirring at 600 rpm. The liquid product obtained in the First Stage comprised of distinct aqueous and organic phases. In each case, the First Stage experiment was carried out four times to obtain sufficient organic phase (first stage upgraded biofuel blend) to maintain the same quantity of feed for the Second Stage. This was important to maintain the same surface to volume ratio in the reactor at the different stages.

After separating the aqueous phase from the organic phase, 60 g of

Table 1
Some properties of the Pt/Al₂O₃ used in this work.

	Specific surface area (m ² /g)	Pore size (nm)	Total pore volume (cm ³ g ⁻¹)
As received Pt/Al ₂ O ₃	166	16.2	0.86
Reduced Pt/Al ₂ O ₃	274	16.1	1.36
Used Pt/Al ₂ O ₃	18.8	8.62	0.37
*Regenerated Pt/Al ₂ O ₃	158	16.2	0.71

*First Stage catalyst regenerated by calcination at 500 °C for 2 h and reduced at 200 °C for 4 h.

Table 2
Fuel properties of final upgraded fuel blend used for engine testing.

Properties	HHV (MJ/kg)	Viscosity at 40°C (cSt/s)	Density (kg/m ³)	Flash point (°C)	Acid value (mgKOH/g)	Cetane number
Bio10FH90	47.69	0.017	691.4	85	0.10	
Kerosene	46.20	0.02	800	48	0.01	49
Diesel	44.10	2.82	832	63		51

the resulting organic phase was introduced into the same reactor for the second stage and reacted with 10 bar H₂ in contact with 5 g of fresh Pt/Al₂O₃ catalyst. The reactor and its contents were heated at 300 °C for 3 h with stirring at 600 rpm. The Second Stage was repeated twice to obtain sufficient organic phase for an optional final stage. Finally, an optional Third Stage was used to refine the combined organic product from the Second Stage by reacting 60 g of it with 10 bar H₂ in contact with a fresh 5 g of the Pt/Al₂O₃ catalyst for 3 h at 300 °C with stirring at 600 rpm. This refining stage was intended to further reduce the oxygen content and promote and hydrogenation and isomerisation, which are desirable to obtain a liquid product comprising mostly of hydrocarbons of fuel quality.

2.3. Analysis of upgrading products

After each stage, the reaction products comprised of gas, liquid and solid residues (spent catalyst and char). The yields gas products were obtained by weighing the reactor before and after discharging the gas from the reactor. A portion of the gas was sampled into a 1 L Tedlar gas bag for analysis using a Shimadzu GC-2014 gas chromatography (GC) fitted with a thermal conductivity detector (TCD) and flame ionisation detector (FID). Detailed description of the GC has been reported previously [22]. The solid products and spent catalysts were recovered via vacuum filtration, dried in an oven at 110 °C for 2 h and weighed. The weight of the solid reaction product (char) was estimated by subtracting the initial weight of catalyst loaded. The aqueous and organic phases were separated on a separating funnel, each phase collected and weighed separately. The organic liquid products were characterised by GC/MS to determine their compositions. The GC/MS used was a Shimadzu model GC-2010 Plus gas chromatograph fitted with a Shimadzu mass spectrometer (model QP2010 SE). The mass selective detector was operated in the electronic impact ionisation mode. The column used was a 30 m length 0.25 mm i.d. SH-Rtx-5MS, supplied by Thames Restek, UK. Oven temperature was maintained at 45 °C for 2.5 min, followed by a first ramp at 2 °C min⁻¹ to 140 °C and held 2 min, and a second ramp at 8 °C min⁻¹ to 280 °C and held for 2.5 min. The injector and transfer line were both held at 280 °C, while a helium carrier gas flow of flow rate of 1 mL min⁻¹ was maintained. The GC/MS data were used to group the compounds in the FP bio-oil. and upgraded fuel blend from each stage into functional groups namely; carboxylic acids, alcohols, ketones, aldehydes, furans, phenols, sugars, esters, ethers and hydrocarbons. The unknown compounds, which were unidentified by the GC/MS were grouped together as “Unknowns”. The dodecane solvent was used as internal standard to quantify the identified compounds. The GC/MS quantification of the FP bio-oil was calculated on dry-ash free (daf) basis to make it comparable to the results of the upgraded organic liquid products. Hence, up to 97 wt% of the upgraded liquid products was quantified, whereas for the FP bio-oil, up to 75.6 wt% (daf) was quantified due to the presence of non-volatile components.

2.4. Testing the thermal stability of dodecane solvent

It is important that the dodecane solvent is not extensively consumed or converted in during the upgrading reactions to ensure any real gains in the process. It would be unwise and uneconomical to consume more

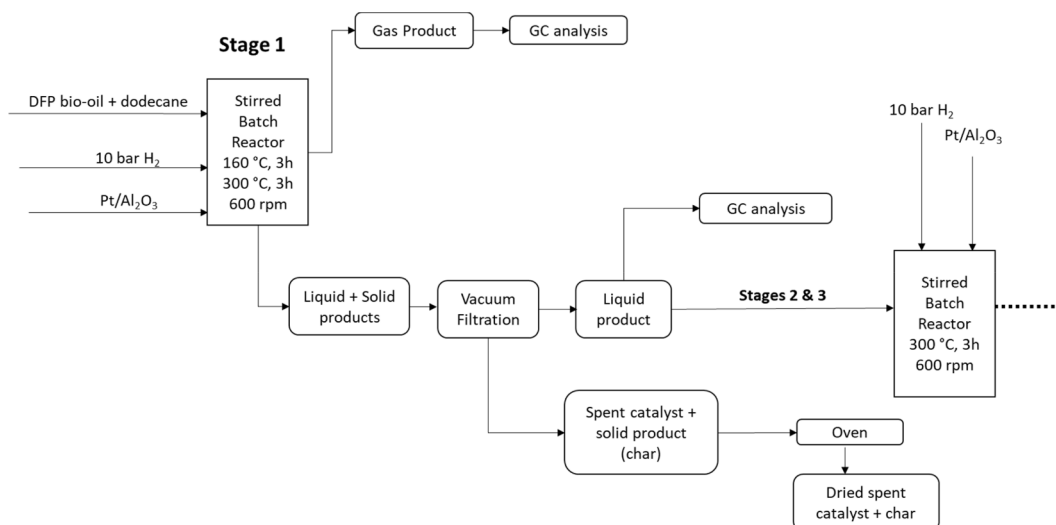


Fig. 1. Schematic of the experimental set-up used in this study (first stage analytical procedures repeated after Stages 2 and 3).

dodecane than the amount of upgraded bio-oil that is eventually produced. Therefore, initial thermal stability tests were carried out on dodecane by reacting the solvent with the Pt/Al₂O₃ through the three stages. The dodecane stability tests were carried out using 36 g of the solvent and 3 g of Pt/Al₂O₃ catalyst at similar conditions used for the actual tests (First Stage: 160 °C for 3 h and then 300 °C for 3 h; Second Stage: 36 g at 300 °C for 3 h; and Third Stage: 36 g at 300 °C for 3 h). In addition, to check the effect of solvent to reactor volume ratio, 60 g of dodecane was heated with 5 g of the catalyst to 300 °C for 6 h and gave similar results (98.8 wt% liquid recovered).

2.5. Combustion and emission characteristics of liquid fuel product

2.5.1. Fuel preparation for engine tests

To carry out the engine tests on the upgraded fuel blend, it was decided to bring the fuel to within the nearest possible biofuel volumes in conventional kerosene and diesel fuels to enable some comparisons of

combustion and emission characteristics. Once the final vol% of biofuel in the upgraded fuel blend was known, a final fuel blend containing the maximum standard biofuel content was made by adding kerosene. Hence, the remaining proportion of final fuel blend used for the engine test consisted of dodecane (from the upgrading process) and the additional kerosene (which contains hydrocarbons around the dodecane range). This final fuel blend for engine test was designated as BioxFHy in this present study; where Bio stands for biofuel, x is the final biofuel vol %, FH stands for fossil hydrocarbon (dodecane and kerosene) and y is their total vol%.

The final upgraded fuel contained 17.6 vol% of biofuel in dodecane and the total volume available for engine test was 1.15 L (i.e., approximately 202.4 mL of biofuel and 947.6 mL of dodecane). The aim was to carry out the engine test with 10 vol% of the biofuel in the final blend. Since, the engine tests required 2 L of fuel, 850 mL diesel was added to make the final test blend with volume compositions as follows: 10.1 vol % biofuel, 47.4 vol% dodecane and 42.5 vol% of kerosene. Since

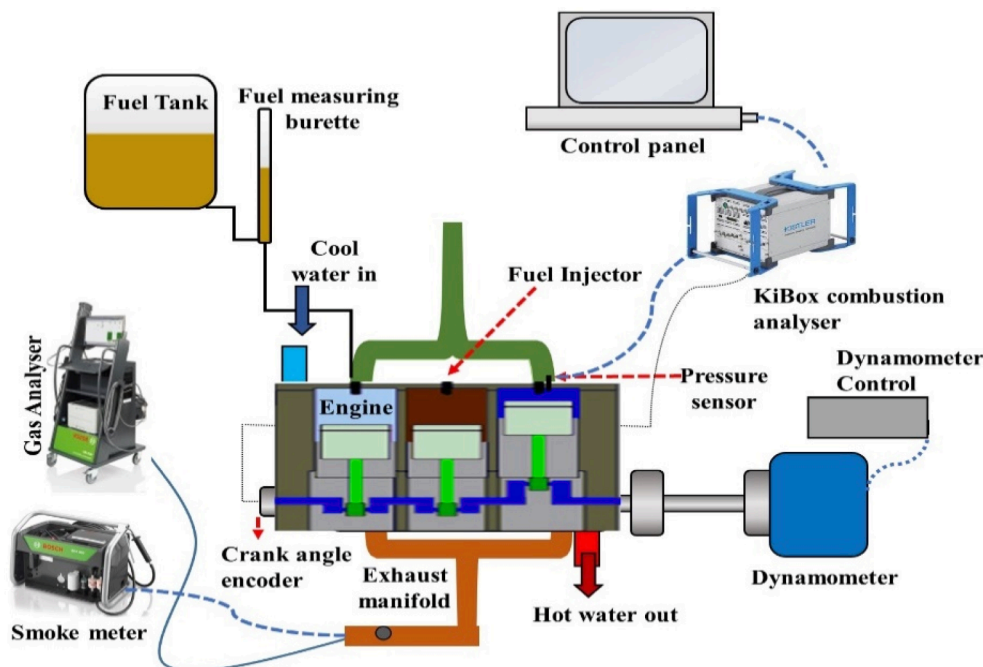


Fig. 2. Schematic of experimental engine test-rig.

dodecane and kerosene were both additional liquid fuels to the biofuel; the final blend for engine tests was designated as Bio10FH90.

2.5.2. Engine test experimental set-up

A three-cylinder, water-cooled, naturally aspirated Lister Petter Alpha series indirect injection (IDI) diesel engine was used for the upgraded fuel blend combustion study, as shown in Fig. 2. Table 3 shows the list of the engine's specifications. While the torque changed, the engine was regulated to keep its speed at 1500 rpm. The engine was loaded with a Froude Hofman AG80HS eddy current dynamometer. For this investigation, five engine loads were employed such as 12, 24, 36, 48 and 60 Nm respectively. A crank angle encoder was mounted on the crankshaft to record the crank angle position, and a Kistler pressure sensor (Kistler 6125C11) was inserted in the cylinder head to record the in-cylinder pressure. Near the head of the fuel injector, a fuel pressure sensor (model Kistler 4618A0 sensor) was installed to the fuel line to measure the fuel line pressure. The Kistler Instruments Ltd.-provided data recorder KiBox was integrated with all three sensors. Utilizing an average of 51 cycles, KiBox combustion software was used to analyse the combustion data and generate in-cylinder pressure, heat release, and fuel injection pressure with respect to crank angle. Engine exhaust gas emissions were measured using a Bosch BEA 850 gas analyser. Table 4 lists the instrument's specifications.

3. Results and discussions

3.1. Thermal stability of dodecane solvent

Results of dodecane thermal stability tests are presented in Table 5, which shows that 99.1 wt% of the dodecane was recovered after the First Stage reactions, with only 0.6 wt% of gas and no solid product. In the Second Stage, the dodecane recovered dropped to 97.5 wt%, with 1.2 wt% of gas formed. No solid product was also formed in the second stage. The Third Stage gave similar results to the second stage, with 98.8 wt% liquid and 1.00 wt% gas and no measurable solid products. GS/MS analysis of the liquid product shown only dodecane as the components, which agrees with its thermal stable under 327 °C [18], and even so in the presence of Pt/Al₂O₃ catalyst. In addition, GC/MS analysis data also confirmed that over 98 wt% of dodecane was recovered when used in the reactions with FP bio-oil, indicating that the solvent was unreactive towards bio-oil under the processing conditions used in this work. Hence, the amount of recovered dodecane from each stage was used to calculate its content in the upgraded biofuel blend.

3.2. Product yields from three-stage processing of FP bio-oil

Using the results of the stability tests for dodecane, the contribution of FP bio-oil to the upgraded biofuel blend and the yield of upgraded biofuel on FP bio-oil basis were calculated using Equation (1):

Mass of biofuel

$$W_{biofuel} = W_{fuel} - (x_{s1} \times x_{s2} \times x_{s3} \times W_{SO}) \quad (1)$$

where W_{fuel} = mass of organic liquid product at each stage; x_{s1}, x_{s2} and x_{s3} = fraction of dodecane recovered in First, Second and Third Stages, respectively (Table 5); and W_{SO} = mass of dodecane in the initial

Table 3
Engine specifications.

Engine model/manufacture	LPWS Bio3/Lister Petter, UK
Number of cylinders	3
Bore/stroke	86 x 88 mm
Cylinder volume	1.395 L
Engine power	9.9 kW @ 1500 rpm
Fuel injection timing	20 deg. bTDC
Compression ratio	22:1

Table 4
Exhaust gas emission analyser specifications.

Emissions	Measuring range	Resolution
CO	0–10 % vol.	0.001 % vol.
CO ₂	0–18 % vol.	0.01 % vol.
HC	0–9999 ppm vol.	1.0 ppm vol.
O ₂	0–22 % vol.	0.01 % vol.
NO	0–5000 ppm vol.	1.0 ppm vol.
Smoke opacity	0–100 %	1 %

Table 5
Results from dodecane thermal stability tests in the presence of Pt/Al₂O₃.

Products	First stage	Second stage	Third stage
Solid (wt%)	–	–	–
Gas (wt%)	0.60 ± 0.12	1.20 ± 0.10	1.00 ± 0.06
Liquid (wt%)	99.1 ± 0.03	97.5 ± 0.02	98.8 ± 0.05
Total balance (wt%)	99.7 ± 0.08	98.7 ± 0.07	99.8 ± 0.05

feedstock. Biofuel yields from each stage can be calculated individually from equation (2).

Therefore, the yields of reaction products over the three stages of the upgrading process are presented in Table 6. The values were obtained using Equation (1):

$$X_{i,j,k} \text{Yield (wt\%)} = \frac{W_{X_{i,j,k}}}{W_{dodecane+bio-oil}} \times 100 \quad (2)$$

where i, j and k represent each of the upgrading Stages (First, Second and Third), respectively. X represents char, aqueous phase, or gas products.

Preliminary First Stage results showed that without the dodecane solvent, char yield was 51.2 wt% from 60 g of bio-oil. If this was extrapolated to the 24 g of bio-oil used in the presence of solvent, the char yield would be 20.4 wt%. With the solvent alone char yield was 18.2 wt%, which was not too different from 20.4 wt% obtained without solvent. However, using 60 g of bio-oil without solvent in the presence of Pt/Al₂O₃ catalyst, a dark tarry material (mixture of char and liquid) that smelt like coal tar was produced, with a combined yield of 67.3 wt%. When both solvent and Pt/Al₂O₃ were used, char yield was 13.6 wt% (a reduction of 33.3 % compared to a corresponding experiment without solvent and catalyst). Therefore, the combination of catalyst, solvent and moderate temperature operation may have prevented excessive char formation, which has been a common challenge during bio-oil upgrading.

After the First Stage, the yield of upgraded biofuel blend was 69.4 wt%. The yield of solid product was 13.6 wt%, which could be deemed to have come entirely from the FP bio-oil. Also, 10.1 wt% of water was obtained at this stage, due to a possible combination of dehydration and hydrogenation reactions of oxygenated compounds in the original FP bio-oil sample [4]. Finally, 6.70 wt% of gas was obtained, which contained unreacted hydrogen gas. Excluding hydrogen gas, the gas product consisted of about 80 % CO₂, 12 % CO, 4 % methane and the rest 4 % comprised of tiny amounts C₂–C₄ hydrocarbon gases. The presence of large amounts on CO₂ in the gas product also indicated that oxygen removal via decarboxylation, for which Pt-based catalysts are known to

Table 6
Percentage yields of products during the three-stage FP bio-oil upgrading process.

Products	First Stage	Second Stage	Third Stage
Solid (wt%)	13.6 ± 0.03	0.85 ± 0.01	0.00 ± 0.00
Gas (wt%)	6.70 ± 0.05	1.12 ± 0.12	1.48 ± 0.02
Oil (wt%)	69.4 ± 0.52	96.5 ± 0.66	98.5 ± 0.14
Water (wt%)	10.1 ± 0.03	1.42 ± 0.02	0.00 ± 0.00
Total balance (wt%)	99.8 ± 0.98	99.9 ± 0.08	100 ± 1.50

be effective [23]. The formation of CO₂ could also be formed from CO via water–gas shift reaction, given presence of water during the reactor.

Hence, the contribution of FP bio-oil after the First Stage was 14.3 wt % or 19.1 vol% (based on density data in Table 7). This corresponded to 24.8 wt% of the initial FP bio-oil feed.

After the Second Stage, 96.5 wt% of liquid product from the First Stage was obtained as organic liquid, along with 1.47 wt% solid, 2.01 wt % gas and 2.49 wt% of water or aqueous phase. Based on the initial feedstock (dodecane and FP bio-oil), the organic liquid yield (upgraded biofuel blend) corresponded to 66.6 wt% yield. The results showed that much of the conversion of the FP bio-oil (deoxygenation, char and gas formation) occurred in the First Stage.

Based on the thermal stability results of dodecane in the Second Stage, the FP bio-oil contributed 13.5 wt% (17.9 vol%) to the upgraded fuel blend. Therefore, the yield of biofuel from the FP bio-oil feed reduced to 22.6 wt%. As shown in Table 6, the optional Third Stage (further refinement) left 98.5 wt% of the second stage liquid product as upgraded fuel blend, while producing 1.48 wt% of gas product. No solid product nor water was obtained at the Third Stage. After the Third Stage, the liquid yield was therefore 66.0 wt% of the starting feedstock (dodecane and FP bio-oil), and with a biofuel content of 13.2 wt% (17.6 vol%). Hence, the final yield of biofuel based on the initial FP bio-oil feed was 21.8 wt%. The final biofuel content is higher than the present blending ratio of in commercial fuels such as 7 (7 vol% biodiesel) and E10 (10 vol% bioethanol). In theory, the complete removal of oxygen (50 wt%) from the FP bio-oil feedstock would give half of the starting weight. However, carbon losses due to decarboxylation, decarbonylation and dealkylation often result in lower yields of upgraded bio-oil, with optimum yield of 19.6 wt% (on dry biomass basis) obtained during continuous processing [14]. Hence, this present study has achieved a similar or better result.

3.3. Characteristics and composition of the FP bio-oil and the upgraded biofuel blends

3.3.1. Physico-chemical characteristics of liquid samples

The overall characteristics of the FP bio-oil starting material, dodecane solvent, conventional kerosene and the product from the Third Stage of the upgrading process i.e., the final upgraded biofuel blend are presented in Table 7. The moisture content of the FP bio-oil was determined to be 29.7 wt%. The oxygen content of the FP bio-oil was 50 wt%, which showed that the FP bio-oil contained half of its weight as oxygen. Considering the 2:3 mass ratio of the bio-oil and dodecane (used as feedstock) in this work, with a theoretical oxygen content of 20 wt%, Table 7 shows that this was reduced to 0.2 wt% (negligible) at the end of the three-stage upgrading process. The oxygen was removed mainly as water (hydrogenation and dehydration; hydro-dehydroxylation), CO₂ (decarboxylation) and CO (decarbonylation).

Whereas the final upgraded fuel blend contained over 13.2 wt% (17.6 vol%) of product derived from the FP bio-oil (Section 3.2), its higher heating value (HHV), elemental compositions as well as H/C molar ratio were similar to those of conventional kerosene but with a small oxygen content (O/C molar ratio of 0.002). In addition, its density is lower than that of kerosene but within similar range. Therefore, the results in Table 7 clearly show reduction in oxygen and water contents from the refining process, as well as the reduction of solids as measured by the ash content on combustion. Hence, the Second Stage product, and certainly the final upgraded fuel blend can be used as a ‘drop in’ replacement for kerosene or diesel fuel, subject to testing of its fuel and emission characteristics (see Section 3.4).

3.3.2. GC/MS compositions of the upgraded biofuel blends

Quantitative analyses of the upgraded biofuel blends obtained from the three stages were carried out by GC/MS with the dodecane solvent as internal standard (Supplementary Information Fig. SI1–SI3). The compositions of these liquid products have been compared to those of the original FP bio-oil in Fig. 3, which shows the changing trends in the

Table 7
Physico-chemical properties of FP bio-oil feedstock, dodecane solvent, final upgraded biofuel blend (product) and conventional kerosene.

	FP bio-oil	Dodecane	*Feedstock (Dodecane + FP bio-oil)	First Stage upgraded fuel blend	Second Stage upgraded fuel blend	Third Stage upgraded fuel blend	Kerosene
Elemental composition							
C (wt%)	43.3 ± 0.3	84.4 ± 0.5	67.0 ± 0.8	83.1 ± 1.3	83.8 ± 0.8	84.7 ± 1.9	84.5 ± 0.5
H (wt%)	6.01 ± 0.6	15.0 ± 0.1	11.4 ± 0.7	14.7 ± 0.5	15.2 ± 0.2	14.6 ± 0.3	15.5 ± 0.5
N (wt%)	0.25 ± 0.01	0.0 ± 0.0	0.08 ± 0.01	0.03 ± 0.7	0.03 ± 0.06	0.02 ± 0.1	0.0 ± 0.0
O (wt%) by difference	50.4 ± 0.7	0.0 ± 0.0	20.2 ± 0.7	2.19 ± 0.3	0.45 ± 0.1	0.19 ± 0.0	0.0 ± 0.0
H/C ratio	1.66	2.13	2.04	2.12	2.18	2.12	2.2
O/C ratio	0.97	0	0.23	0.02	0.004	0.002	0
Other properties							
Ash (%)	1.52 ± 0.25	nd	0.62	nd	nd	nd	nd
HHV (MJ/Kg)	21.44 ^a	47.84 ^a	37.3	41.84	42.31	46.97 ^a	46.20 ^b
Water content (%)	29.7 ± 0.8	nd	11.9 ± 0.8	0.6 ± 0.2	0.6 ± 0.2	0.5 ± 0.2	nd
Acid number (mgKOH/g)	166.1	nd	66.4	1.36	0.8	0.38	nd
pH value	2.4 ± 0.3	n/a	n/a	n/a	n/a	n/a	n/a
Density (kg/m ³) at 25 °C	1300	749	960	810	780	752	800
Flash Point (°C)	166	73	nd	nd	nd	72	48
Viscosity at 40 °C (cSt)	98	1.36	nd	nd	nd	1.23	1.32

*Calculated based on immiscible feedstock composition (40 wt% FP bio-oil + 60 wt% dodecane); a = Calculated using the Kistler Instruments Ltd (Hampshire, UK) KiBox (RTM) powertrain analysis system; b = Literature data; nd = not determined; n/a = not applicable.

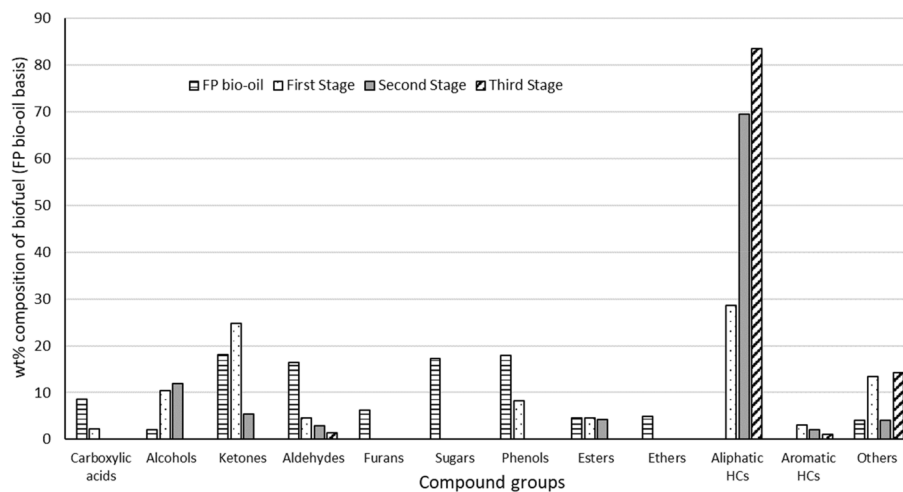


Fig. 3. Percentage compositions upgraded biofuel blends from the three stages compared to the FP bio-oil.

proportions of the various groups of compounds. Fig. 3 shows that certain compound groups found in the FP bio-oil such as sugars, furans and ethers disappeared completely after the First-Stage processing. After the First Stage, the proportions for ketones increased and while aliphatic and aromatic hydrocarbons appeared in the upgraded product (Supplementary Information Table SI2). Extensive deoxygenation (through the formation of water and char formation were observed during this First Stage (Table 5) as well as CO₂ release. After the Second Stage, Fig. 3 shows that the proportion of all other compound groups in the upgraded biofuel (liquid) product decreased, while aliphatic hydrocarbons increased dramatically by a factor of 1.43 compared to the First Stage. These changes in compositions of the upgraded fuel blend (Supplementary Information Table SI3) indicate the increased deoxygenation of the fuel in the presence of catalyst and moderate hydrogen pressure (only 10 bar).

These trends continued up to the third stage, so that aliphatic hydrocarbon accounted for nearly 84 % of the upgraded product. It should be noted here that alkanes and cycloalkanes accounted for over 98 % of the aliphatic hydrocarbons (Supplementary Information Table SI4). These results agree with the data in Table 7, which showed that the final product possessed similar or slightly better physico-chemical properties than dodecane and conventional kerosene. For example, Table 7 shows that the viscosity of the final upgraded fuel was 1.23 cP, which is lower than those of kerosene (1.32 cP) and dodecane (1.36 cP). This could be attributed to the presence of shorter chain alkanes and cycloalkanes present in the upgraded fuel (Supplementary Information Table SI4). Certain compounds were unidentified by the GC/MS, however, giving the low oxygen contents of the Third-Stage organic liquid product (final upgraded fuel blend), those compounds could be deemed to be hydrocarbons.

Preliminary tests via X-ray diffraction (XRD) analysis showed that the catalyst crystalline phases changed dramatically First Stage due mainly to char formation on catalyst surface and hydrolysis of the gamma-alumina support for form boehmite ($\text{Al}_2\text{O}_3 + \text{H}_2\text{O} \rightarrow 2\text{AlO}(\text{OH})$) (Supplementary Information Figure SI4). This could be attributed to the presence of large amounts of water formed during the First Stage. Therefore, the main deactivation mechanisms could be hydrolysis and coke formation. However, the properties of the recovered and recalined First Stage catalysts were similar to those of fresh catalyst (Table 1), which indicated the possibility of catalyst regeneration. Detailed study on the stability of the catalysts over repeated cycles for the three stages will be undertaken as part of future work.

3.4. Engine combustion analysis

For any CI engine, the combustion process normally involves both premixed combustion and diffusion burning. The choice of fuel, injection time, temperature, intake pressure, compression ratio, and engine load are some of the variables that can have an impact on the mechanics of these complicated phenomena [24–26]. The primary factor affecting engine performance and exhaust emissions is how effectively the combustion process occurs. The next discussion will go over significant combustion process factors such ignition delay (ID), combustion duration (CD), in-cylinder gas pressure and heat release rate during the combustion of Bio10FH90 fuel, kerosene and diesel.

3.4.1. Start of combustion (SoC) and end of combustion (EoC) analysis

The start of combustion (SoC) is taken at a crank angle of 5 % of the total heat released by the fuel, and the end of combustion (EoC) is taken at 90 % of the total heat released by the fuel [27]. The start of injection (SoI) is constant at 20 °CA bTDC for all the tested fuels. From Fig. 4 (a), it is observed that SoC for Bio10FH90 lies between kerosene and diesel fuel due to differences in the fuel properties (Tables 2 and 6). SoC decreased with increased engine load due to rising in-cylinder temperature which enhanced the vapourisation and fuel/air mixing rate [27,28]. The cetane numbers (CN) for kerosene and diesel are 49 and 51, respectively, meaning that CN of tested Bio10FH90 lies between them. Already the H/C molar ratio of Third Stage upgraded fuel blend (2.12) is slightly lower but close to that of kerosene (2.20) in Tables 2 and 6; hence Bio10FH90 should have even much closer H/C ratio to kerosene. This concludes that CN Bio10FH90 has been improved by adding 10 % upgraded fuel blend in kerosene. The SoC of diesel fuel is 0.96 °CA, which is higher than that of kerosene. Whereas Bio10FH90 blend was found 0.55 °CA advanced and 0.41 °CA retarded compared to kerosene and diesel fuel at lower BMEP (0.99 bar). The slight oxygen availability and equivalent H/C molar ratio to kerosene (Table 6) in upgraded fuel blend enhanced the combustion process and retarded the SoC (Fig. 4a). The SoC of Bio10FH90 was retarded by 0.10 °CA, 0.08 °CA and 0.13 °CA compared to diesel fuel and 1 °CA, 0.7 °CA, 0.8 °CA compared to kerosene at BMEP 2 bar, 2.99 bar and 3.97 bar, respectively. At full engine load (BMEP 4.95 bar), the difference in SoC was observed to be negligible due to higher in-cylinder temperature and better combustion. The EoC extended with increases in the engine load due to increases in the amount of fuel to maintain the constant speed (1500 rpm) (Fig. 4b). The overall EoC for Bio10FH90 was found to be from 0.4 to 1.9 °CA shorter than kerosene and 0.4–2.7 °CA shorter than diesel fuel. However, EoC for kerosene was observed between 1.4 and 3.2 °CA. Overall observation of EoC shows that the difference was in the optimal range.

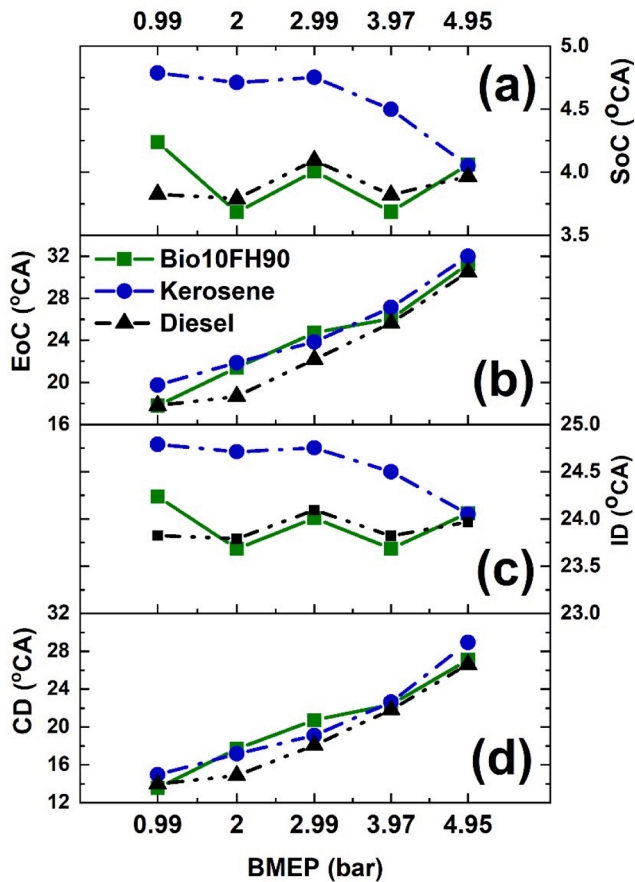


Fig. 4. Results of combustion analyses of tested fuels: (a) SoC, (b) EoC, (c) ID and (d) CD.

3.4.2. Ignition and combustion analysis

The physical and chemical delays make up most of the factors that affect the ignition delay (ID) time [27,29]. The pre-combustion processes in the fuel/air combination cause the chemical delay, whereas atomization, mixing, and vaporisation are responsible for the physical delay [30]. With an increase in BMEP, the engine's ignition delay gets shorter. This is brought on by a rise in gas temperature inside the cylinder, which shortens the time needed for physical ignition. Fig. 4 (c) depicts how the ignition delay varies for each of the test fuels in relation to BMEP. The ID of Bio10FH90 and kerosene were observed to be higher than fossil diesel fuel at all BMEPs, due to lower CN which retarded the SoC. ID for Bio10FH90 fuel was found 0.5°CA shorter than kerosene and 0.4°CA longer than diesel fuel at lower BMEP (0.99 bar). The ID period for Bio10FH90 was observed to be 0.1°CA, 0.08°CA, and 0.13°CA shorter than diesel fuel and 1°CA, 0.7°CA and 0.8°CA shorter as compared to kerosene at BMEP 2 bar, 2.99 bar and 3.97 bar. But at full engine load (BMEP 4.9 bar), ID period for Bio10FH90 was observed slightly higher than kerosene and fossil diesel (Fig. 4c). Lower CN fuel take longer time to ignite at low engine load (Fig. 4a), due to lower in-cylinder temperature [31,32]. At medium BMEP, engine global cylinder temperature was increase which reduced the ID period for Bio10FH90 (Fig. 4c). The combustion duration (CD) increases with engine load [31,32]. CD for Bio10FH90 was observed lower 10% and 3% than kerosene and diesel fuels at 0.99 bar BMEP. But it increased by 3% and 16% at BMEP 2 bar, 7% and 12% at BMEP 2.99 bar as compared to kerosene and diesel fuels (Fig. 4d). Whereas it also observed that CD for Bio10FH90 further decreased by 1% and 6% than kerosene at 3.97 bar and 4.95 bar BMEP. When compared with diesel fuel at higher BMEP (3.97 bar & 4.95 bar), CD for Bio10FH90 blend was found 2.4% and 1.7% higher. Overall longer CD is observed for Bio10FH90, the reason would

be different hydrocarbon present in Bio10FH90 (ascribed to Fig. 3) which take more time to breakdown in smaller molecule to burn completely [30,33]. Second reason would be a short ID of Bio10FH90 which is known to increase the premix-combustion duration and extend the diffusion combustion duration [16,29].

3.4.3. In-cylinder pressure and heat release rate

The engine's in-cylinder pressure data may be used to examine the power output and emissions efficiently [34,35]. The percentage of fuel that is consumed during the early stage of combustion affects the peak cylinder pressure of a diesel engine [36]. The ability of the fuel and air to combine is demonstrated by the cylinder pressure. Fig. 5 (a-e) depicts the fluctuation in cylinder pressure with respect to crank angle for tested fuels at different engine load conditions and constant speed 1500 rpm. The maximum cylinder pressure (Pmax) for Bio10FH90, kerosene and diesel fuel were observed 62.79 bar at 11.8°CA aTDC, 61.93 bar at 14°CA aTDC and 65 bar at 11°CA aTDC at lower BMEP (0.99 bar), 63.28 bar at 12.9°CA aTDC, 63.17 bar at 11.3°CA aTDC and 64.34 bar at 13.4°CA aTDC at medium BMEP (2.99 bar) and 67.32 at 11.5°CA aTDC, 65.86 bar at 10.8°CA aTDC and 67.16 bar at 12.9°CA aTDC at full load condition (BMEP 4.95 bar). It is observed that Bio10FH90 shows lower peak pressure at low and medium BMEPs (0.99 bar, 2 bar and 2.99 bar) than diesel fuel but higher than kerosene at all BMEP. Whereas Pmax for Bio10FH90 increased at higher BMEP (3.97 bar and 4.95 bar) as compared to diesel fuel as shown in Fig. 6(a). Pmax for the kerosene was found between Bio10FH90 and diesel fuel at all the BMEPs (Fig. 6a). Pmax for Bio10FH90 blend was observed 1.3% higher than kerosene and 2% lower than diesel fuel at lower BMEP 0.99 bar. Pmax for Bio10FH90 found 1.6% and 0.09% higher than kerosene and diesel fuel at BMEP 2 bar; 0.16% higher than kerosene and 1.6% lower than diesel fuel at 2.99 bar BMEP; 2.9% and 0.32% higher than kerosene and diesel fuel and 2.1% and 0.24% higher than kerosene and diesel fuel at full load (BMEP 4.95 bar). It is observed that Pmax for Bio10FH90 blend and kerosene was lower than diesel fuel due to lower CN. Lower CN fuel give longer ID period which take more time to make combustible mixture this results lower Pmax [37,38]. As engine load increased, the duration of ID was reduced, and more fuel get burn to produce more in-cylinder pressure [37,38].

Figure 5 (a-e) shows the variation of heat release rate (HRR) for all the tested fuels at different BMEP. The lower CN and longer CD reduced the HRR [39]. It can be clearly observed from the curves that kerosene produced higher HRR at low BMEP (0.99 bar). This could be due to lower CN, low in-cylinder temperature and longer CD but HRR for kerosene reduced with increasing the engine load (Fig. 5a). The maximum heat release rate (HRRmax) for Bio10FH90 was observe 15% lower than kerosene and 1.7% higher than diesel fuel at 0.99 bar BMEP (Fig. 6b). As load increase, HRRmax for Bio10FH90 reduced by 9% and 13% at 2 bar BMEP, 32.4% and 5.5% at 2.99 bar BMEP and 4% and 10% at full load (4.95 bar BMEP) compared to kerosene and diesel fuels, respectively. In addition, HRR for Bio10FH90 increased by about 15% and 7% more than kerosene and diesel fuels, respectively at 3.97 bar BMEP. Moreover, Bio10FH90 showed lower HRR at 0.9 bar BMEP than kerosene due to lower in-cylinder temperature and shorter ID. HRR for Bio10FH90 increased with engine load due to increasing engine cylinder temperature [37,40]. Higher in-cylinder temperature reduces the physical delay and enhances the fuel vapourisation and air/fuel mixing rate [41]. This allows more fuel to burn during combustion [41]. This may be linked to the slightly superior O/C and equivalent H/C molar ratios of the Bio10FH90, which improved the combustion efficiency. Therefore, HRR for bio-oil was observed higher than kerosene and diesel at 3.97 bar BMEP. At full engine load (4.95 bar BMEP), engine cylinder temperature slightly reduced due to rich fuel mixture and insufficient time for complete combustion which results lower HRRmax for Bio10FH90 (Fig. 5e and Fig. 6b).

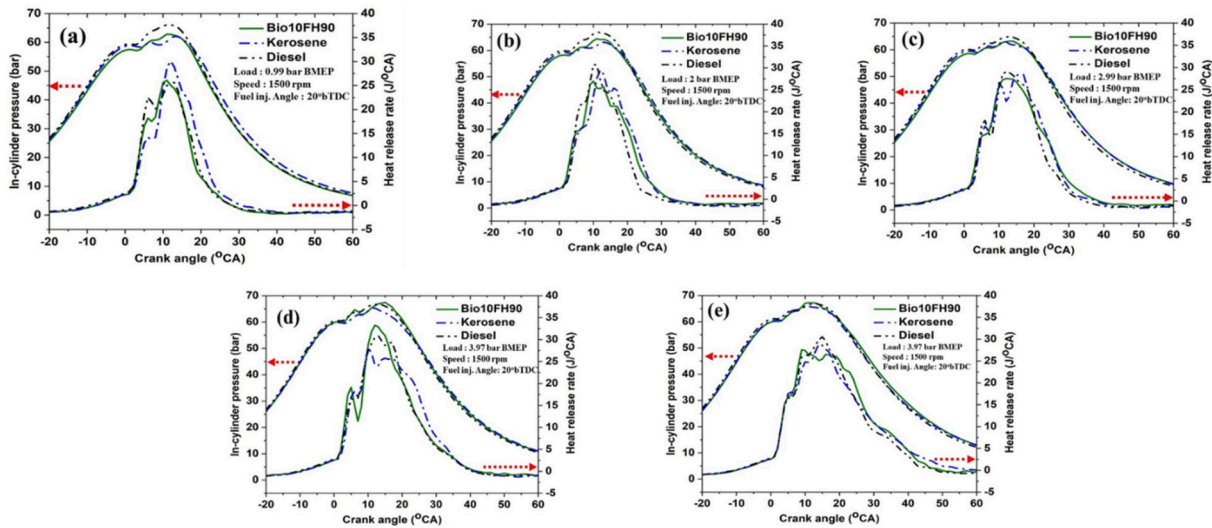


Fig. 5. Cylinder pressure and hear release rate (HRR) variation with respect to crank angle.

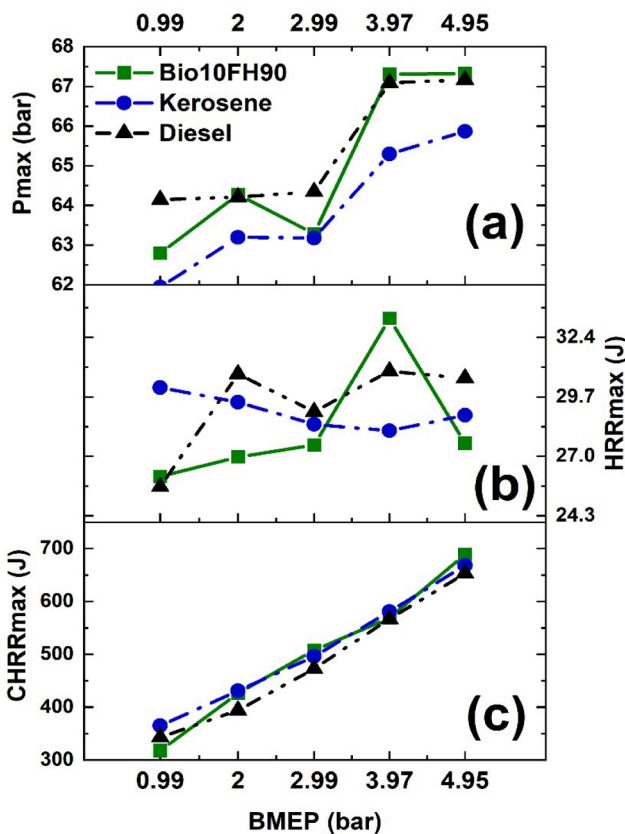


Fig. 6. (a) Maximum pressure (Pmax), (b) heat release rate (HRRmax) and (c) cumulative heat release (CHRRmax) vs BMEP.

3.4.4. Cumulative heat release rate (CHRR)

The effect of Bio10FH90 with respect to kerosene and diesel fuel on cumulative heat release rate (CHRR) at various BMEP is shown in Fig. 7. CHRR curve shows better understanding about total heat energy produced by the fuel during combustion [27]. Bio10FH90 and kerosene showed higher CHRR in comparison to diesel fuel due to their slightly higher calorific value (HHV) of kerosene (46 MJ/kg) compared to diesel (42.6 MJ/kg) At 0.99 bar BMEP, Bio10FH90 shows lower CHRR than kerosene due to lower CV and in-cylinder temperature but higher than

diesel fuel due to higher CV than diesel. With further increases in the engine load, CHRR for Bio10FH90 moved closer to that of kerosene at BMEP 2 bar, 2.99 bar and 3.97 bar. Whereas, at full load (4.95 bar BMEP) CHRR for Bio10FH90 was observed to be higher than kerosene and diesel fuel, which may be due to the lower density of the Bio10FH90 compared to the other fuels. CHRR for kerosene was reduce at full load due to rich fuel mixture, most of the fuel molecules did not get enough oxygen to make a combustible mixture and lack of insufficient time for combustion. Maximum cumulative heat released rate (CHRRmax) for Bio10FH90 was lower by 14 % and 7 %, respectively at 0.99 bar BMEP as compared to kerosene and diesel fuel (Fig. 6c). Whereas CHRRmax for Bio10FH90 was 1 % lower than kerosene and 7 % higher than diesel fuel at 2 bar BMEP. At full engine load (4.95 bar BMEP), CHRRmax for Bio10FH90 increased by 3 % and 5 % as compared to kerosene and diesel fuel (Fig. 6c).

3.5. Engine performance analysis

The Fig. 8 shows how the brake specific fuel consumption (BSFC) varies with respect to different engine loads for all tested fuels. BSFC is the ratio between the amounts of fuel consumed by the engine to the amount of brake power produced by the engine [42]. Generally, it can be seen that the BSFC reduced with the engine load increment irrespective of the fuel combination up to medium load and then, it slightly rose due to increasing fuel-rich mixtures [43,44]. This is because the excess amount of power requirement at high loads is achieved by the lower amount of fuel [43,44]. The lower the specific fuel consumption, higher the efficiency of the engine and fuel used. BSFC for Bio10FH90 was observed to be lower than kerosene and diesel fuel at all BMEP due to lower density and higher HHV. BSFC for Bio10FH90 was 16 % and 9 % at 0.99 bar BMEP, 13.2 % and 13.4 % at 2 bar BMEP, 23 % and 28 % at 2.99 bar BMEP, 10 % and 12 % at 3.97 bar BMEP and 5 % and 10 % at full load (4.95 bar BMEP) as compared to kerosene and diesel fuel. Brake thermal efficiency (BTE) refers to how much chemical energy in the fuel is converted into useful energy. Different results of thermal efficiency values concerning engine load are shown in Fig. 8. It is observed that the BTE for diesel fuel was lower due to lower HHV and higher BSFC, whereas Bio10FH90 shows higher BTE about 11 % and 2 % at 0.99 bar BMEP, 8 % and 0.6 % at 2 bar BMEP, 16 % and 12 % at 2.99 bar BMEP, 6 % and 0.17 % at 3.97 bar BMEP and 2 % and 1.6 % at full load (4.95 bar BMEP) as compared to kerosene and diesel fuel. Higher BTE for Bio10FH90 could be due to higher HHV and availability of oxygen. This fuel bound oxygen improve the air/fuel ratio and enhance the overall combustion efficiency [43,44].

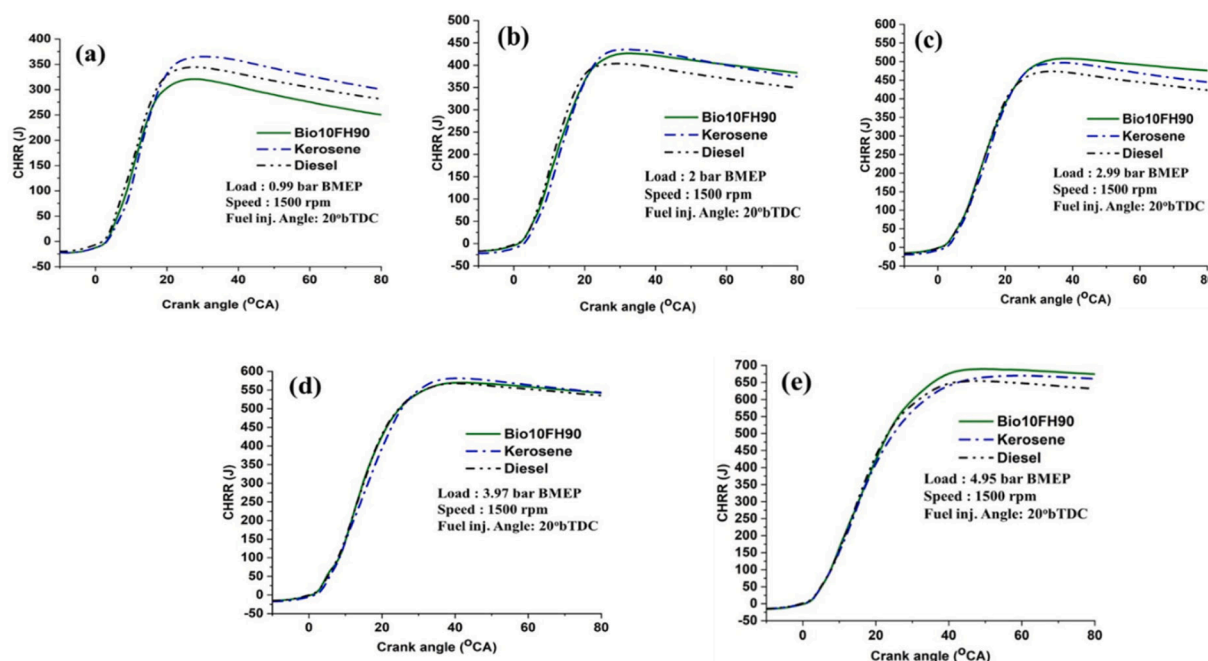


Fig. 7. Cumulative heat release rate (CHRR) variation.

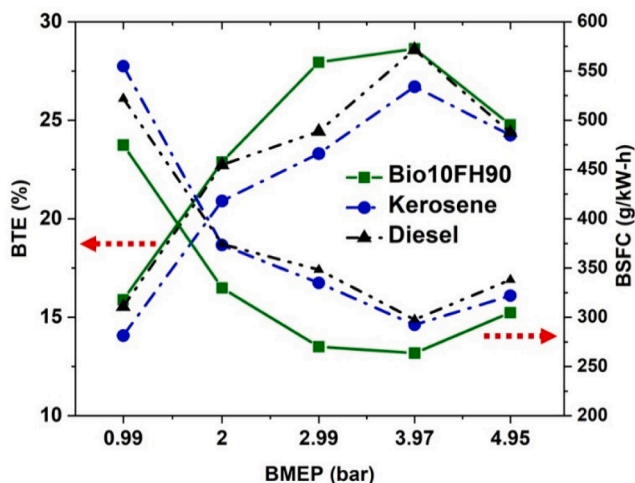


Fig. 8. Engine performance analysis – BTE and BSFC.

3.6. Exhaust emission analysis

3.6.1. CO and CO₂ emissions

The emissions of CO are mainly caused by incomplete combustion of fuels through the combustion chamber [42]. Variations in CO emissions of all fuel types tested are shown in Fig. 9(a). Fig. 9(a) shows that CO emissions decreased with increasing engine load up to medium load condition of 2.9 bar BMEP due to fuel-lean mixture. But it rose at higher load (BMEP 3.97 bar & 4.95 bar) due to the prevalent rich fuel-rich mixture, shorter time for combustion that led to incomplete combustion of carbon. CO emission for Bio10FH90 fuel was observed to be lower by 50 %, 33 % and 50 % at 0.99 bar, 3.97 bar and 4.95 bar BMEP than kerosene, whereas it was similar to kerosene at 2 bar and 2.99 bar BMEP. When compared to diesel fuel, Bio10FH90 produced 42 %, 75 % and 25 % CO lower than diesel fuel at 0.99 bar, 2 bar and 4.95 bar BMEP, respectively. In addition, CO for Bio10FH90 was observed to be equivalent to diesel fuel at 2.99 bar and 3.97 bar BMEP, respectively. The lower CO for Bio10FH90 may be due to its relatively higher oxygen

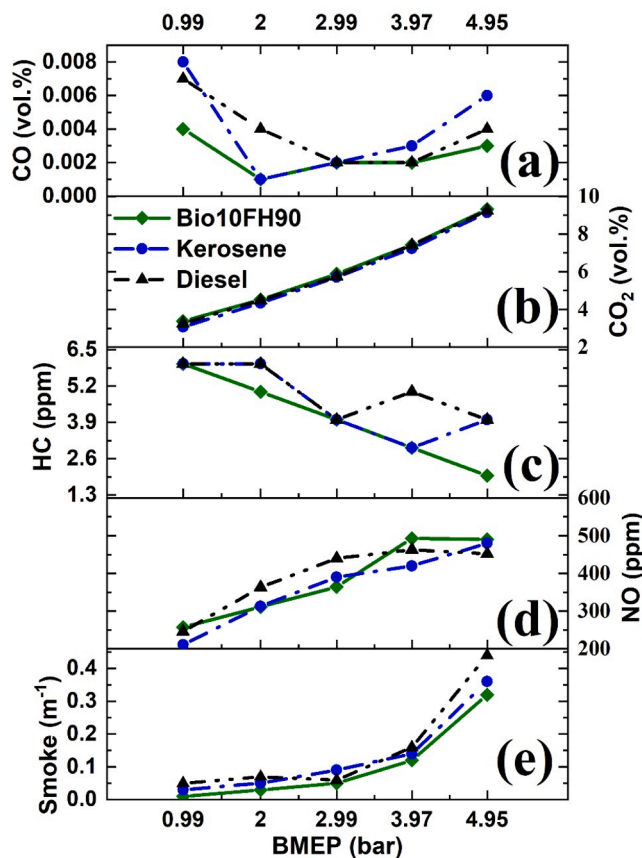


Fig. 9. Emissions formation (a) CO, (b) CO₂, (c) HC, (d) NO and (e) Smoke with respect to BMEP.

content compared to kerosene and diesel, which increased the oxidation rate of CO to CO₂ [36]. In addition, the presence of light hydrocarbons within the C₇ – C₁₁ range (Supplementary Information Table S11) in Bio10FH90, may have made it a cleaner burning fuel.

Carbon dioxide (CO₂) emissions are the inevitable result of the complete combustion of carbon in the fuel [45]. Fig. 9(b) shows the different concentrations of CO₂ emissions for all tested fuel at different loads. It can be observed that CO₂ increased with increasing engine loads and was higher for Bio10FH90 compared to kerosene and diesel fuels. The CO₂ emissions for Bio10FH90 were higher by about 10 % and 3.6 % at 0.99 bar BMEP, 4 % and 0.8 % at 2 bar BMEP, 3 % and 2 % at 2.99 bar BMEP, 2.4 % and 0.13 % at 3.97 bar BMEP and 1.7 % and 0.7 % at full load (4.95 bar BMEP) when compared to kerosene and diesel fuels, respectively. Bio10FH90 possessed slightly higher O/C molar ratio but more importantly, was a seemingly lighter fuel due to its content of lighter alkanes; the combination of these two factors may have enhanced its rate of combustion and oxidation to CO₂ with the rise in-cylinder temperature at full load.

3.6.2. Hydrocarbon emissions

HC emissions are mainly formed due to incomplete combustion of fuel. It is one of the most important parameters in defining the nature of combustion [46]. Fig. 9(c) shows that HC emissions decreased with increasing engine loads. It was observed that Bio10FH90 gave lower HC emissions than kerosene and diesel, respectively, possibly due to its relatively higher oxygen content and the presence of lighter hydrocarbons. As compared to kerosene, Bio10FH90 showed 16 % and 50 % lower HC emissions at 0.2 bar and 4.95 bar BMEP (full load) whereas, it behaved similarly to kerosene at 0.99 bar, 2.99 bar, and 3.97 bar, respectively. When compared to diesel fuel, Bio10FH90 showed 16 %, 50 % and 40 % lower at 2 bar, 3.97 bar and 4.95 bar BMEP and equivalent at 0.99 bar and 2.99 bar BMEP. Overall, it was observed that Bio10FH90 gave better combustion efficiency than the samples of the two conventional samples tested in this study.

3.6.3. Nitric oxide emissions

Nitric oxide (NO) emissions are formed mainly due to the abundance of oxygen and the high temperature of the combustion chamber [37,45,47]. NO emissions are very harmful emissions to the environment, which hinders the improvement of engines. The higher the combustion quality, the higher the temperature, and the greater the NO formation [37,45,47]. Fig. 9(d) shows the different NO concentrations in the exhaust gases for the different fuels. Bio10FH90 showed higher NO emissions at lower BMEP (0.99 bar) about 17 % and 4 % than kerosene and diesel, respectively, due to its lower in-cylinder temperature and longer ID [47]. Even though, ID for Bio10FH90 was observed to be longer than that of kerosene but its properties (e.g. small oxygen content, lower density) made combustion better [47]. At medium load, NO formation for bio-oil blend was lower by 0.6 % and 16 % at 2 bar BMEP and 7 % and 20 % at 2.99 bar BMEP than kerosene and diesel, respectively. The lower NO formation for Bio10FH90 at medium BMEP was due to shorter ID and low P_{max}. The shorter ID reduced the duration of pre-mix combustion by allowing less fuel to burn and extend the diffusion combustion. The formation of NO emissions for Bio10FH90 was increased by 14 % and 6 % at 3.97 bar BMEP and 2 % and 7.7 % at 4.95 bar BMEP as compared to kerosene and diesel, respectively. NO emissions for Bio10FH90 increased at higher load due to high in-cylinder temperature and rich O/C ratio.

3.6.4. Smoke emission

The variation of smoke density produced during the test for different fuels is presented in Fig. 9(e). The smoke density increases with an increase in brake power of the engine, since smoke vastly depends on the engine load [46]. Smoke emission is a visible indicator of the incomplete combustion due to the presence of fuel-rich mixture at full load condition [46]. It was observed that smoke emissions for Bio10FH90 was decreased by 66 % and 80 % at 0.99 bar BMEP, 40 % and 57 % at 2 bar BMEP, 44 % and 16 % at 2.99 bar BMEP, 14 % and 24 % at 3.97 bar BMEP and 11 % and 27 % at full load (4.95 bar BMEP) as compared to kerosene and diesel, respectively. Results therefore showed that that

smoke opacity for Bio10FH90 blend was significantly decreased relative to the other fuels tested in this work.

4. Conclusion

In this present study, an upgraded fuel blend consisting of 13.2 wt% biofuel was produced through a novel solvent-assisted catalytic upgrading process and further blended to make a final fuel for combustion and emissions tests in a conventional diesel engine.

A three-stage bio-oil catalytic upgrading process was developed using 5 wt% Pt/Al₂O₃ catalyst and dodecane (as solvent) to minimise char formation. Detailed GC/MS analysis of organic liquid products showed the extent of deoxygenation through the stages, leading to the third-stage final liquid product with a high-content of green hydrocarbons (from GC/MS analyses) and very low oxygen (0.2 wt%) content. Considering that the FP bio-oil feedstock contained 50.4 wt%, oxygen complete deoxygenation would reduce the biofuel yield to half of its original mass (without carbon loss); therefore obtaining 21.8 wt% on FP bio-oil basis, was arguably, one of the highest biofuel yields from upgrading of bio-oil ever reported in literature. This upgraded fuel blend gave physico-chemical properties similar to those of conventional kerosene.

Extensive combustion and emission tests revealed of the final fuel blend, containing 10 vol% biofuel ((Bio10FH90) gave an overall better engine performance than kerosene and diesel fuels. It gave improved the combustion characteristics such as early SoC and shorter ID than kerosene. Bio10FH90 produced lower in-cylinder pressure rise and P_{max} than diesel but higher than kerosene Bio10FH90 produced high HRR 15 % and 7 % than kerosene and diesel at 3.97 bar BMEP but it slightly reduced at full load due fuel-rich mixture. Overall gross heat release rate for bio-oil was found higher than the kerosene and diesel fuel due to better % of C/O and C/H. Bio10FH90 shows higher BTE 2 % and 1.6 % than kerosene and diesel and lower BSFC. Bio10FH90 showed overall better engine emissions; CO was lower for Bio10FH90 by 50 % and 25 % than kerosene and diesel fuel due to presence of small amounts of oxygenates as well as lighter alkanes and cycloalkanes from the upgraded fuel, giving higher CO₂. This higher in-cylinder temperature also enhanced NO formation. NO emissions for Bio10FH90 increased from 2–14 % at full engine load as compared to kerosene and diesel fuels. In contrast, HC and smoke emissions were observed to be lower by 16–50 % and 16–40 %, respectively from the upgraded fuel blend compared to kerosene and diesel. An indirect injection (IDI) type engine was used in this study as IDI type engine is more suitable for bio-oil blends. Testing this developed blend on advanced engine combustion test rig with different operating conditions will be within the scope of future research work. Overall investigation of the Bio10FH90 fuel blend showed that it could be used as transportation fuel for heavy vehicles, aviation (Jet engine) and marine application.

Funding

This work was supported by Innovate UK Energy Catalyst Round 7 Early Stage (Grant No 38286).

CRedit authorship contribution statement

Jude A. Onwudili: Conceptualization, Methodology, Project administration, Resources, Supervision, Investigation, Validation, Visualization, Writing – original draft, Writing – review & editing. **Vikas Sharma:** Methodology, Investigation, Formal analysis, Writing – original draft. **Cristiane Almeida Scaldaferrri:** Investigation, Methodology, Data curation, Formal analysis, Validation. **Abul K. Hossain:** Methodology, Supervision, Validation, Visualization, Validation, Writing – review & editing.

Declaration of Competing Interest

The authors declare that they have no known competing financial interests or personal relationships that could have appeared to influence the work reported in this paper.

Data availability

Data will be made available on request.

Acknowledgements

The authors would like to thank the Energy & Bioproducts Research Institute (EBRI) and Aston University, UK for all support received.

Appendix A. Supplementary data

Supplementary data to this article can be found online at <https://doi.org/10.1016/j.fuel.2022.127028>.

References

- [1] Statistical Review of World Energy, 70th Edition. 2021 <https://www.bp.com/content/dam/bp/business-sites/en/global/corporate/pdfs/energy-economics/statistical-review/bp-stats-review-2021-full-report.pdf>. 2022 [Accessed: July 1, 2022].
- [2] Roser HR and M. Energy 2020. <https://ourworldindata.org/energy-archive.2022> [Accessed: August 1, 2022].
- [3] U.S. Energy Information Administration (EIA). Annual Energy Review 2011. <https://www.eia.gov/totalenergy/data/annual/pdf/aer.pdf> 2022, [accessed August 10, 2022].
- [4] Schmitt CC, Raffelt K, Zimina A, Krause B, Otto T, Rapp M, et al. Hydrotreatment of fast pyrolysis bio-oil fractions over nickel-based catalyst. *Top Catal* 2018;61:1769–82. <https://doi.org/10.1007/s11244-018-1009-z>.
- [5] Bridgewater AV. Review of fast pyrolysis of biomass and product upgrading. *Biomass Bioenergy* 2012;38:68–94. <https://doi.org/10.1016/j.biombioe.2011.01.048>.
- [6] Feroso J, Pizarro P, Coronado JM, Serrano DP. Advanced biofuels production by upgrading of pyrolysis bio-oil WIREs. *Energy Environ* 2017;6:1–18. <https://doi.org/10.1002/wene.245>.
- [7] Khan MS, Ra M, Sookrah V, Thomson MJ. Effect of dewatering wood-derived fast pyrolysis oil on its fuel properties for power generation. *Energy Fuels* 2019;33:12403–20. <https://doi.org/10.1021/acs.energyfuels.9b00802>.
- [8] Huber GW, Iborra S, Corma A. Synthesis of transportation fuels from biomass: Chemistry, catalysts, and engineering. *Chem Rev* 2006;106:4044–98. <https://doi.org/10.1021/cr068360d>.
- [9] Vanderauwera PFLP, Wambeke DMC. Valorisation of bio-oil resulting from fast pyrolysis of wood. *Chemical* 2014;68:1205–12. <https://doi.org/10.2478/s11696-014-0541-y>.
- [10] Bilbao R, Santos JM, Melo JA, Bene M, Wisniewski A, Fonts I. Hydrodeoxygenation of lignocellulosic fast pyrolysis bio-oil: characterization of the products and effect of the catalyst loading ratio. *Energy Fuels* 2019. <https://doi.org/10.1021/acs.energyfuels.9b00265>.
- [11] Zacher AH, Olarte MV, Santosa DM, Elliott DC, Jones SB. A review and perspective of recent bio-oil hydrotreating research. *Green Chem* 2014;4:491–515. <https://doi.org/10.1039/c3gc41382a>.
- [12] Wang H, Lee S, Olarte MV, Zacher AH. Bio-oil stabilization by hydrogenation over reduced metal catalysts at low temperatures. *ACS Sustain Chem Eng* 2016;4:5533–45. <https://doi.org/10.1021/acssuschemeng.6b01270>.
- [13] Kadarwati S, Oudenhoven S, Schagen M, Hu X, Garcia-Perez M, Kersten S, et al. Polymerization and cracking during the hydrotreatment of bio-oil and heavy fractions obtained by fractional condensation using Ru/C and NiMo/Al₂O₃ catalyst. *J Anal Appl Pyrolysis* 2016;118:136–43. <https://doi.org/10.1016/J.JAAP.2016.01.011>.
- [14] Zia Abdullah, Brad Chadwell, Rachid Taha, Barry Hindin KR. Final Technical Report: Upgrading of Bio-Oil Produced by Pyrolysis 2015. <https://www.osti.gov/servlets/purl/1209232>. 2022 (accessed August 1, 2022).
- [15] Szwaja M, Chwist M, Szymank A. Pyrolysis oil blended n-butanol as a fuel for power generation by an internal combustion engine. *J Energy* 2022;261:125339. <https://doi.org/10.1016/j.energy.2022.125339>.
- [16] Rajamohan S, Suresh S, Mallinathan S, Harigopal A, Nhand Nguyen V, Engel D, et al. Optimization of operating parameters for diesel engine fuelled with bio-oil derived from cottonseed pyrolysis. *Sustain Energy Technol Assessments* 2022;52:102202. <https://doi.org/10.1016/J.SETA.2022.102202>.
- [17] Midhun Prasad K, Murugavel S. Experimental investigation and kinetics of tomato peel pyrolysis: Performance, combustion and emission characteristics of bio-oil blends in diesel engine. *J Clean Prod* 2020;254:120115. <https://doi.org/10.1016/J.JCLEPRO.2020.120115>.
- [18] Zhou P, Crynes BL. Thermolytic reactions of dodecane. *Ind Eng Chem Process Des Dev* 1986;25:508–14. <https://doi.org/10.1021/i200033a027>.
- [19] Checa M, Marinas A, Marinas JM, Urbano FJ. Deactivation study of supported Pt catalyst on glycerol hydrogenolysis. *Applied Catal A Gen* 2015;507:34–43. <https://doi.org/10.1016/j.apcata.2015.09.028>.
- [20] Li X, Gunawan R, Wang Y, Chaiwat W, Hu X, Gholizadeh M, et al. Upgrading of bio-oil into advanced biofuels and chemicals. Part III. Changes in aromatic structure and coke forming propensity during the catalytic hydrotreatment of a fast pyrolysis bio-oil with Pd/C catalyst. *Fuel* 2014;116:642–9. <https://doi.org/10.1016/j.fuel.2013.08.046>.
- [21] Elkasabi Y, Mullen CA, Pighinelli ALMT, Boateng AA. Hydrodeoxygenation of fast-pyrolysis bio-oils from various feedstocks using carbon-supported catalysts. *Fuel Process Technol* 2014;123:11–8. <https://doi.org/10.1016/j.fuproc.2014.01.039>.
- [22] Razaq I, Simons KE. Parametric Study of Pt/C-Catalysed Hydrothermal Decarboxylation of Butyric Acid as a Potential Route for Biopropane Production *Energies* 2021;14:3316. 10.3390/en14113316.
- [23] Lopez-Ruiz JA, Davis RJ. Decarbonylation of heptanoic acid over carbon-supported platinum nanoparticles. *Green Chem* 2014;16:683–94. <https://doi.org/10.1039/c3gc41287c>.
- [24] Vélez Godiño JA, Torres García M, Jiménez-Espadafor Aguilar FJ. Experimental analysis of late direct injection combustion mode in a compression-ignition engine fuelled with biodiesel/diesel blends. *Energy* 2022;239. <https://doi.org/10.1016/j.energy.2021.121895>.
- [25] Kanth S, Ananad T, Debbarma S, Das B. Effect of fuel opening injection pressure and injection timing of hydrogen enriched rice bran biodiesel fuelled in CI engine. *Int J Hydrogen Energy* 2021;46:28789–800. <https://doi.org/10.1016/j.ijhydene.2021.06.087>.
- [26] Singh D, Sharma D, Soni SL, Inda CS, Sharma S, Sharma PK, et al. A comprehensive review of physicochemical properties, production process, performance and emissions characteristics of 2nd generation biodiesel feedstock: *Jatropha curcas*. *Fuel* 2021;285:119110. <https://doi.org/10.1016/j.fuel.2020.119110>.
- [27] Rezk A, Sharma V, Hossain AK, Ahmed A. Study on using graphene and graphite nanoparticles as fuel additives in waste cooking oil biodiesel. *Fuel* 2022;328:125270. <https://doi.org/10.2139/ssrn.4073454>.
- [28] Zhang X, Lan Chi NT, Xia C, Khalifa AS, Brindhadevi K. Role of soluble nano-catalyst and blends for improved combustion performance and reduced greenhouse gas emissions in internal combustion engines. *Fuel* 2022;312:122826. <https://doi.org/10.1016/J.FUEL.2021.122826>.
- [29] Chakraborty A, Biswas S, Meitei S, Sengupta A. Examining the significance of the ignition characteristics of hydrogen and liquefied-petroleum-gas on the reactivity controlled compression ignition and its interspersed profiles induced in an existing diesel engine: a comparative perspective. *Energy Convers Manage* 2022;268:115976. <https://doi.org/10.1016/j.enconman.2022.115976>.
- [30] Bai Y, Wang Y, Wang X, Zhou Q, Duan Q. Development of physical-chemical surrogate models and skeletal mechanism for the spray and combustion simulation of RP-3 kerosene fuels. *Energy* 2021;215:119090. <https://doi.org/10.1016/J.ENERGY.2020.119090>.
- [31] Thakkar K, Kachhwaha SS, Kodgire P, Srinivasan S. Combustion investigation of ternary blend mixture of biodiesel/n-butanol/diesel: CI engine performance and emission control. *Renew Sustain Energy Rev* 2021;137:110468. <https://doi.org/10.1016/j.rser.2020.110468>.
- [32] Sharma V, Duraisamy G, Arumugam K. Impact of bio-mix fuel on performance, emission and combustion characteristics in a single cylinder DIC VCR engine. *Renew Energy* 2020;146:111–24. <https://doi.org/10.1016/J.RENENE.2019.06.142>.
- [33] Bayındır H, Işık MZ, Argunhan Z, Yücel HL, Aydın H. Combustion, performance and emissions of a diesel power generator fueled with biodiesel-kerosene and biodiesel-kerosene-diesel blends. *Energy* 2017;123:241–51. <https://doi.org/10.1016/J.ENERGY.2017.01.153>.
- [34] Ağbulut Ü, Polat F, Sarıdemir S. A comprehensive study on the influences of different types of nano-sized particles usage in diesel-bioethanol blends on combustion, performance, and environmental aspects. *Energy* 2021;229:120548. <https://doi.org/10.1016/J.ENERGY.2021.120548>.
- [35] Emma AF, Alangar S, Yadav AK. Extraction and characterization of coffee husk biodiesel and investigation of its effect on performance, combustion, and emission characteristics in a diesel engine. *Energy Convers Manage X* 2022;14:100214. <https://doi.org/10.1016/j.ecmx.2022.100214>.
- [36] Gad MS, Ismail MA. Effect of waste cooking oil biodiesel blending with gasoline and kerosene on diesel engine performance, emissions and combustion characteristics. *Process Saf Environ Prot* 2021;149:1–10. <https://doi.org/10.1016/J.PSEP.2020.10.040>.
- [37] Sharma V, Hossain AK. Experimental Investigation of Neat Biodiesels' saturation level on combustion and emission characteristics in a CI engine. *Energies* 2021;14:5203. <https://doi.org/10.3390/en14165203>.
- [38] Patil V, Thirumalini S. Effect of cooled EGR on performance and emission characteristics of diesel engine with diesel and diesel-karanja blend. *Mater Today Proc* 2021;46:4720–7. <https://doi.org/10.1016/J.MATPR.2020.10.303>.
- [39] Sharma V, Ganesh · D. Combustion and emission characteristics of reformulated biodiesel fuel in a single-cylinder compression ignition engine. *Int J Environ Sci Technol* 2020;17:243–52. 10.1007/s13762-019-02285-8.
- [40] Jayabal R, Thangavelu L, Subramani S. Combined effect of oxygenated additives, injection timing and EGR on combustion, performance and emission characteristics of a CRDi diesel engine powered by sapota biodiesel/diesel blends. *Fuel* 2020;276:118020. <https://doi.org/10.1016/j.fuel.2020.118020>.
- [41] Patel C, Chandra K, Hwang J, Agarwal RA, Gupta N, Bae C, et al. Comparative compression ignition engine performance, combustion, and emission characteristics, and trace metals in particulates from Waste cooking oil, *Jatropha*

- and Karanja oil derived biodiesels. *Fuel* 2019;236:1366–76. <https://doi.org/10.1016/j.fuel.2018.08.137>.
- [42] Baweja S, Trehan A, Kumar R. Combustion, performance, and emission analysis of a CI engine fueled with mustard oil biodiesel blended in diesel fuel. *Fuel* 2021;292:120346. <https://doi.org/10.1016/j.fuel.2021.120346>.
- [43] Uyumaz A, Aydoğan B, Yılmaz E, Solmaz H, Aksoy F, Mutlu İ, et al. Experimental investigation on the combustion, performance and exhaust emission characteristics of poppy oil biodiesel-diesel dual fuel combustion in a CI engine. *Fuel* 2020;280:118588. <https://doi.org/10.1016/j.fuel.2020.118588>.
- [44] Sharma V, Duraisamy G, Cho HM, Arumugam K, Alosius MA. Production, combustion and emission impact of bio-mix methyl ester fuel on a stationary light duty diesel engine. *J Clean Prod* 2019;233:147–59. <https://doi.org/10.1016/J.JCLEPRO.2019.06.003>.
- [45] Mourad M, Mahmoud KRM, NourEldeen ESH. Improving diesel engine performance and emissions characteristics fuelled with biodiesel. *Fuel* 2021;302:121097. <https://doi.org/10.1016/j.fuel.2021.121097>.
- [46] Du J, Su L, Zhang D, Jia C, Yuan Y. Experimental investigation into the pore structure and oxidation activity of biodiesel soot. *Fuel* 2022;310:122316. <https://doi.org/10.1016/j.fuel.2021.122316>.
- [47] Kumar Kadian A, Khan M, Sharma RP, Mozammil hasnain SM. Performance enhancement and emissions mitigation of DI-CI engine fuelled with ternary blends of jatropha biodiesel-diesel-heptanol. *Mater Sci Energy Technol* 2022;5:145–54. [10.1016/j.mset.2022.01.002](https://doi.org/10.1016/j.mset.2022.01.002).